Joint Impact of Forecast Tendency and State Error Biases in Ensemble Kalman Filter Data Assimilation of Inner-Core Tropical Cyclone Observations

TOMISLAVA VUKICEVIC

Hurricane Research Division, NOAA/Atlantic Oceanographic and Meteorological Laboratory, Miami, Florida

ALTUĞ AKSOY

Hurricane Research Division, NOAA/Atlantic Oceanographic and Meteorological Laboratory, and Cooperative Institute for Marine and Atmospheric Studies, University of Miami, Miami, Florida

PAUL REASOR AND SIM D. ABERSON

Hurricane Research Division, NOAA/Atlantic Oceanographic and Meteorological Laboratory, Miami, Florida

KATHRYN J. SELLWOOD

Hurricane Research Division, NOAA/Atlantic Oceanographic and Meteorological Laboratory, and Cooperative Institute for Marine and Atmospheric Studies, University of Miami, Miami, Florida

FRANK MARKS

Hurricane Research Division, NOAA/Atlantic Oceanographic and Meteorological Laboratory, Miami, Florida

(Manuscript received 30 July 2012, in final form 23 January 2013)

ABSTRACT

In this study the properties and causes of systematic errors in high-resolution data assimilation of inner-core tropical cyclone (TC) observations were investigated using the Hurricane Weather Research and Forecasting (HWRF) Ensemble Data Assimilation System (HEDAS). Although a recent study by Aksoy et al. demonstrated overall good performance of HEDAS for 83 cases from 2008 to 2011 using airborne observations from research and operational aircraft, some systematic errors were identified in the analyses with respect to independent observation-based estimates. The axisymmetric primary circulation intensity was underestimated for hurricane cases and the secondary circulation was systematically weaker for all cases. The diagnostic analysis in this study shows that the underestimate of primary circulation was caused by the systematic spindown of the vortex core in the short-term forecasts during the cycling with observations. This tendency bias was associated with the systematic errors in the secondary circulation, temperature, and humidity. The biases were reoccurring in each cycle during the assimilation because of the inconsistency between the strength of primary and secondary circulation during the short-term forecasts, the impact of model error in planetary boundary layer dynamics, and the effect of forecast tendency bias on the background error correlations. Although limited to the current analysis the findings in this study point to a generic problem of mutual dependence of short-term forecast tendency and state estimate errors in the data assimilation of TC core observations. The results indicate that such coupling of errors in the assimilation would also lead to short-term intensity forecast bias after the assimilation for the same reasons.

1. Introduction

Over the last two decades, there has been a marked improvement in prediction of tropical cyclone (TC) tracks, while forecasting intensity has remained a major challenge with virtually no improvement (Rappaport et al. 2009; Berg and Avila 2011). Recognizing that mesoscale processes play a critical role in TC evolution (Montgomery and Smith, 2011; Emanuel 2005), high-resolution numerical weather prediction (NWP) models have been employed to study improvements to the TC intensity forecast. The positive impact of high resolution

Corresponding author address: Tomislava Vukicevic HRD, NOAA/AOML, 4301 Rickenbacker Causeway, 7451 SW 133rd St., Miami, FL 33156.
E-mail: tomislava.vukicevic@noaa.gov

DOI: 10.1175/MWR-D-12-00211.1

on the intensity forecast was demonstrated in studies by Gopalakrishnan et al. (2002), Gopalakrishnan et al. (2006), X. Zhang et al. (2011), Davis et al. (2008), and Gopalakrishnan et al. (2011). In addition, Xiao et al. (2009), Weng and Zhang (2012), and F. Zhang et al. (2011) demonstrated that assimilation of high-resolution Doppler radar wind observations within the TC core region could significantly improve the forecast skill of high-resolution models. More generally, these results indicate that reducing the uncertainty in the mesoscale aspects of the initial conditions could have a significant positive impact on the skill of TC intensity prediction with high-resolution models (Gall et al. 2013).

In this study, we focus on the systematic errors (the biases) in vortex-scale ensemble Kalman filter (EnKF) data assimilation. Although initial condition uncertainty is typically associated with random errors, because these errors are traditionally considered for determining the predictability limit (Lorenz 1969; Rotunno and Snyder 2008), systematic errors could have a stronger influence on the prediction skill and may limit predictability to shorter time scales than would be associated with the random error growth. Studies by Weng and Zhang (2012) and F. Zhang et al. (2011) have provided examples of impact of systematic errors in the initial condition for the TC intensity forecast problem. In these studies the forecast skill improvement from the EnKF assimilation of Doppler radar observations in the vortex-scale initial condition was demonstrated using the deterministic forecasts that were initialized by the mean analyses. Because the initial systematic errors were reduced in the mean analysis by design, relative to a state without data assimilation, the deterministic forecast skill improvement is directly attributed to reducing these errors. Also, the ensemble forecast results in Weng and Zhang (2012) exhibited similar skill improvement to the deterministic forecast, further suggesting the influence of reduced bias in the initial condition. It is interesting that the forecasts in both studies exhibited much lower skill improvement within first 12–24 h than at a longer range. Such result suggests that the systematic errors, which affected the short-term forecast, were either not reduced or could have been introduced during the data assimilation. Overall, the prior studies point to the importance of addressing the systematic errors in the mesoscale initial conditions for the TC intensity prediction with high-resolution models.

In this study, we investigate possible causes of the systematic errors in high-resolution EnKF data assimilation at TC vortex scales. Specifically, the results of data assimilation experiments presented in Aksoy et al. (2013) with the Hurricane Weather Research and Forecasting (HWRF) Ensemble Data Assimilation System (HEDAS; Aksoy et al. 2012) were analyzed. In this analysis special attention was given to a mutual dependence of the short-term forecast biases and the systematic errors in the assimilation. The evaluation of the impact of the HEDAS analyses on the forecast after data assimilation is presented in Gall et al. (2013). A brief summary of HEDAS and the data assimilation results in Aksoy et al. (2013) that are relevant to the analysis in this study are presented in section 2. The methodology of diagnostic analysis of the systematic errors in the assimilation is described in section 3. The results are summarized in section 4. Conclusions are presented in section 5.

2. Data assimilation system and application to cases from 2008 to 2011 hurricane seasons

a. HEDAS

HEDAS was developed at the Hurricane Research Division of the National Oceanic and Atmospheric Administration (NOAA) Atlantic Oceanographic and Meteorological Laboratory (AOML) to assimilate TC inner-core observations for high-resolution vortex initialization (Aksoy et al. 2012, 2013). The observations assimilated with this system include airborne Tail Doppler Radar (TDR) radial wind speed, stepped-frequency microwave radiometer surface wind speed, and flight-level and dropwindsonde measurements from research and operational aircraft (Aberson 2010; Aberson et al. 2006). These observations are routinely transmitted in real time and therefore are available for potential assimilation into operational models.

As described in Aksoy et al. (2012, 2013) HEDAS is based on a serial implementation of the square root EnKF of Whitaker and Hamill (2002). In a serial update loop, each observation is treated as a scalar quantity, using a simplified version of the update equations of Whitaker and Hamill (2002). The simplification was based on Eqs. (4)–(7) in Snyder and Zhang (2003). Three-dimensional, distance-dependent covariance localization, using a compactly supported fifth-order correlation function following Gaspari and Cohn (1999) was applied. In the application with TC vortex observations the localization length scale was chosen so that most of the vortex is updated given the limited spatial distribution of observations.

In the assimilation, the experimental version of the HWRF model (Gopalakrishnan et al. 2002, 2006; X. Zhang et al. 2011) was configured with a horizontal grid spacing of 9 and 3 km on the outer and inner domains, respectively. The vortex-following nest motion of the inner domain was suppressed during the assimilation and all ensemble members were initialized with collocated

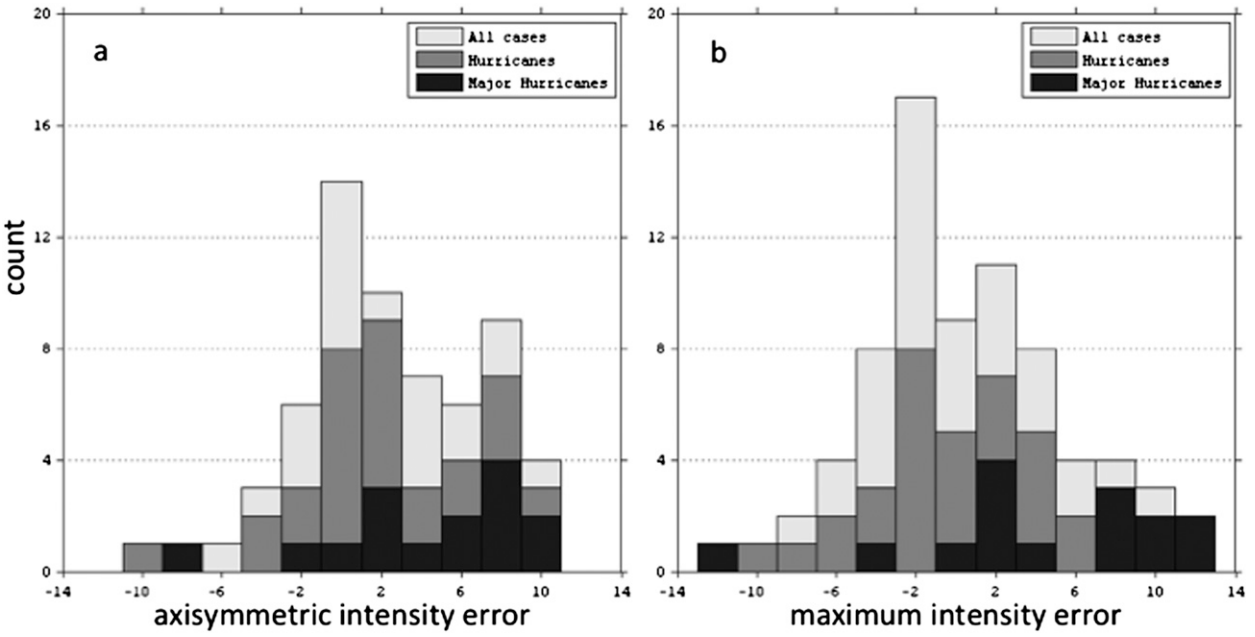

FIG. 1. Frequency distribution of primary circulation intensity errors (observed − analysis) in the final HEDAS analysis for 83 cases [the cases are described in Aksoy et al. (2013) study]. Units are m s^{-1}. (a) Maximum amplitude of axisymmetric flow at height of 1 km and (b) maximum wind speed at height of 10 m with respect to independent 3D Doppler wind analysis and the best-track estimate. All 83 cases (light gray), all hurricane intensity cases (dark gray), and major hurricanes greater than category 2 (black).

inner domains to facilitate gridpoint-based spatial covariance computations in the EnKF. The inner grid domain size was about 10° × 10° in latitude and longitude. The forecast ensemble comprised 30 members. The initial and lateral boundary ensemble perturbations were obtained from the experimental, EnKF-based global ensemble prediction system developed for the National Centers for Environmental Prediction (NCEP) Global Forecast System (GFS). The details of this system and its performance for the prediction of 2009 and 2010 tropical cyclones are summarized in Hamill et al. (2011a,b). An ensemble spinup was carried out for 3–4 h prior to the data assimilation. These ensemble forecasts were initialized 6 h prior to the synoptic time around which a respective NOAA P-3 flight was centered. The serial assimilation of observations included 2–7 hourly cycles, depending on the case. Further technical details of HEDAS and the associated HWRF model configuration are included in Aksoy et al. (2012, 2013).

b. Systematic errors in the final HEDAS analysis

The real data experiments with HEDAS for 83 cases of observed TCs from 2008–11 are presented in detail in Aksoy et al. (2013). In this section the results that are relevant to the systematic error analysis in the current study are summarized.

Aksoy et al. (2013) showed that overall HEDAS produced a realistic analysis in terms of TC center position and primary circulation intensity, axisymmetric vertical and radial structure, as well as first-order vortex asymmetry. However, the analysis, for the cases with an observed intensity higher than tropical storm strength exhibited a systematic underestimate (the negative bias) of the axisymmetric primary circulation intensity relative to an independent wind analysis based on TDR observations using the three-dimensional variational Doppler analysis technique (Gamache 1997; Reasor et al. 2009). Although the amplitude of the systematic error was not large when averaged over all cases, it was significant. This is evident from the error frequency diagram in Fig. 1a, which shows that the amplitude of axisymmetric tangential wind speed error was larger than 6 m s^{-1} for about 45% of the hurricane intensity cases. An intensity error of this amplitude is 2–3 times larger than the expected error variance of the TDR wind observations and the Doppler-based analysis of the axisymmetric primary circulation (Reasor et al. 2009; Rogers et al. 2012). In addition, Aksoy et al. (2013) show that the amplitude of azimuthal wavenumber 1 in the primary circulation exhibited a negative bias (lower amplitude) relative to the Doppler-based wind analysis (Fig. 13b in Aksoy et al. 2013).

Similar to the axisymmetric primary circulation, estimates of the maximum sustained wind speed at 10 m, a standard measure of TC intensity (Rappaport et al. 2009), exhibited significant negative bias (lower intensity) with

respect to the best-track estimates for the cases of observed intensity greater than Saffir–Simpson category 2 (hurricane wind scale, National Hurricane Center, http://www.nhc.noaa.gov). The error frequency diagram for the maximum intensity errors is displayed in Fig. 1b. As may be expected, the maximum intensity and axisymmetric primary circulation intensity errors were positively correlated. However, the results in Fig. 1 show that the latter errors had less bias for the lower intensity hurricane cases. This result could be attributed to the discrepancy between temporal and spatial scales of the maximum intensity in the model and observations, implying the presence of more random errors.

The secondary circulation in the analysis also exhibited systematic errors both in intensity and structure. Aksoy et al. (2013) show that the maximum amplitude of axisymmetric radial inflow in the analysis had a large negative bias (lower amplitude) relative to the Doppler-based analysis; whereas the inflow depth exhibited a positive bias (deeper than observed). Regarding the temperature field, the analysis was characterized by a notable bias relative to the assimilated flight level observations. The sign and strength of this bias was dependent on the storm intensity. A significant positive temperature bias (warmer than observed), of about 3 K, was associated with cases that had observed intensity less than or equal to Saffir–Simpson category 2 hurricane strength, whereas a smaller amplitude but significant negative bias was characteristic of the major hurricane cases. Similar results were obtained for the humidity analysis, which exhibited significant positive bias for the lower intensity storms and a slight negative bias for the major hurricane cases, most notably in the vortex eye region.

In summary, the inspection of systematic errors in the final HEDAS analyses reveal some biases in the estimates of vortex primary and secondary circulation for the hurricane intensity cases relative to independent analyses using the same TDR observations. Given that these observations constituted ~99% of the observations in the analysis, and that the Doppler-based analyses of the axisymmetric primary circulation have a negligible bias (Reasor et al. 2009; Rogers et al. 2012), the results suggest that the background forecast bias was the primary cause of the systematic errors in the primary circulation analysis. A similar conclusion applies to the analysis of the secondary circulation with the caveat that the Doppler-based analysis of this circulation is characterized by larger uncertainties than the primary circulation as a result of the properties of observations (Gamache 1997). The systematic errors in the temperature and humidity, relative to the flight-level observations that were assimilated, also suggest strong influence of the background forecast bias in the assimilation.

TABLE 1. Cases used in the analysis. The intensity is from the NHC's best-track estimate.

Case index	Storm name	Verification time	Intensity ($m\,s^{-1}$)	Assimilation interval (h)
1	Earl	1200 UTC 29 Aug 2010	33.4	3 + 6
2	Earl	0000 UTC 30 Aug 2010	43.7	3 + 5
3	Earl	1200 UTC 30 Aug 2010	54.0	3 + 6
4	Earl	0000 UTC 31 Aug 2010	59.1	3 + 6
5	Earl	1200 UTC 1 Sep 2010	56.6	3 + 6
6	Earl	0000 UTC 2 Sep 2010	61.7	3 + 6
7	Earl	1200 UTC 2 Sep 2010	59.1	3 + 5
8	Earl	0000 UTC 3 Sep 2010	46.3	3 + 6
9	Bill	0000 UTC 10 Aug 2009	54.0	3 + 7
10	Gustav	1200 UTC 30 Aug 2008	54.0	3 + 5

3. Method of diagnostic analysis

The relationship between the short-term forecast and data assimilation was evaluated in terms of the evolution of kinematic and mass fields during sequential updating (cycling) of the state by HEDAS (Aksoy et al. 2012, 2013). The diagnostic analysis was performed using the prior (forecast) and posterior (analysis) state quantities in the vortex-relative coordinate system. Eight cases for Hurricane Earl (29 August–3 September 2010), and two single cases for Hurricanes Bill (19 August 2009) and Gustav (30 August 2008) were included (Table 1). The Hurricane Earl cases captured several periods of evolution, from the tropical storm to major hurricane intensity, including periods of rapid intensification, quasi–steady state, and decay before extratropical transition. The Hurricane Bill and Gustav cases were selected as additional examples of periods of intensification from hurricane-strength storms to major hurricanes.

For the vortex-relative diagnostics, the prior and posterior state at each analysis update was first transformed into cylindrical coordinates with height-varying location of the vortex center. The vortex centers were computed for each state and level independently using a vorticity-centric search algorithm. The state transformation was performed by a linear interpolation of three-dimensional wind and mass fields from the model native georeferenced grid onto the vortex-centric cylindrical grid consisting of 300 radial and 360 azimuthal coordinates with spacing of 1 km and 1°, respectively. The vertical levels considered in the analysis were as follows: 0.01, 0.05, 0.4, 0.6, 0.8, 1, 2, 3, 4, 6, 8, and 10 km. The variables used in the analysis

were as follows: tangential, radial, and vertical wind speed (denoted v, u, and w, respectively), temperature (denoted T), specific humidity (denoted q), and minimum sea level pressure (MSLP). The following primary diagnostics were computed using these variables:

1) Maximum of azimuthally averaged (i.e., the axisymmetric) values of v at each vertical level, denoted $\max(V_t)$. This diagnostic represents a measure of intensity of the vortex primary circulation within the eyewall region.
2) Maximum of v at each vertical level at any grid point, denoted $\max(v)$.
3) Radius of maximum wind at each vertical level, denoted rmw. This radius is defined as the radial distance of $\max(V_t)$ from the vortex center.
4) Axisymmetric radial wind at vertical levels within the PBL, averaged within the radial interval $1.5\text{rmw} \geq r \geq 1\text{rmw}$. This diagnostic is denoted V_{r*} and represents a measure of strength of the radial component of the secondary circulation in the vortex core.
5) Axisymmetric $w > 0$ at each level, averaged within radial interval, $1.5\text{rmw} \geq r \geq 1\text{rmw}$. This diagnostic is denoted $\max(W)$ and represents a measure of strength of the vertical component of the secondary circulation associated with convection in the eyewall region. Conversely, this diagnostic is a measure of the convective activity in this region.
6) Radius–height fields of the axisymmetric wind components (V_t, V_r, and W).
7) Depth of the inflow layer, defined here as the average height at which the radial wind changes sign from negative to positive. The average was computed in azimuth and within the radial interval $1.5\text{rmw} \leq r \leq 1.0\text{rmw}$. This diagnostic is denoted h_{PBL}.

These diagnostics were computed for the prior ensemble mean state and posterior mean analysis in each cycle during the assimilation. As described in section 2, the assimilation period consisted of 3 h of so-called spinup from the initial condition that was derived from the interpolated global ensemble analysis, followed by 4–7 analysis cycles, each spanning a 1-h interval, depending on the case. The diagnostics of the prior mean states included the forecasts prior to the data assimilation period, resulting in total of 7–10 diagnostic values, depending on the case. The number of diagnostic analysis cycles for each case is shown in Table 1.

In addition to the mean state diagnostics, the properties of ensemble-based background error correlations were evaluated. As is well known, in EnKF data assimilation, the background error covariance directly impacts the state update by the observations. This covariance represents a statistical estimate of the first-order, or linear, relationship between variations in the state that result from the state evolution during the short-term ensemble forecast. As such, the background error covariance include the effect of forecast model representation of dynamical processes and the associated model errors. Consequently, the properties of background error correlations could aid in diagnosing the sources of background forecast error. In the current analysis, the error correlations were computed in the vortex-relative framework. This approach facilitated the interpretation of the forecast errors in terms of vortex dynamics without the influence of location errors. Although the location errors could have an important contribution to the background error covariance in the analysis updates, especially in the early cycles as shown in the study by Poterjoy and Zhang (2011), they would have negligible influence on the dynamic errors within the vortex, assuming the vortex environment was similar among the ensemble members. This assumption was satisfied in the experiments with HEDAS because of the use of a fixed inner grid location and a short forecast interval of 1 h. The assumption would not be valid for the cases with a strong influence from surface variability such as in the presence of land. The diagnostic analysis in this study did not include such cases.

For the error correlation analysis, the prior state of axisymmetric wind components (V_t, V_r, and W), temperature (T), and humidity (Q), and MSLP were first computed for each ensemble member, resulting in an ensemble of two-dimensional (2D) variables in the r–z-mean coordinate system. The radial coordinate was then normalized by the radius of maximum wind at each level and independently for each ensemble member. In this way, the axisymmetric state of each ensemble member was represented in the same coordinate system for the computation of correlations.

The analysis of correlations was primarily focused on the relationship between variations of the primary circulation and other variables. For this purpose, the error correlation function was represented by a set of vertical profiles of correlations between $\max(V_t)$ at a fixed location (r^*, z^*) and another variable $X(r, z)$ at several vertical levels, including z^*. The set consisted of the vertical profiles for different radial locations for $X(r, z)$. Each axisymmetric variable (V_t, V_r, W, T, and Q) was used for X. The representation of error correlations in terms of the vertical profiles was used for ease of examining the vertical coupling of variations within the vortex. The error correlation diagnostics are discussed in section 4b.

4. Analysis of systematic errors in the assimilation

a. Evolution of mean state in the data assimilation cycling

1) PRIMARY CIRCULATION

For the cases of Hurricane Earl in which the final HEDAS analysis produced a significant underestimate of storm intensity with respect to the best-track estimate and the Doppler-based wind analysis (the cases 4–7 in Table 1), the evolution of max(V_t) and max(v) in Fig. 2 indicates that in each cycle the intensity of the primary circulation systematically weakened at all heights in the short-term forecast after the increase in the preceding analysis update. In most cycles, the decline of the primary circulation intensity in the forecast was similar in amplitude to the increase in the analysis update, especially when the increase was large. Such error in the forecast led to virtually no net gain of the primary circulation intensity in the assimilation. This result points to a bias in forecast tendency in the form of spindown of the entire primary circulation in the vortex core during the assimilation for the hurricane intensity cases.

The vortex spindown occurred also during the period prior to the data assimilation (the first three instances of forecast in Fig. 2) for the same cases, relative to the initial condition that was provided by the global ensemble analysis. These analyses already contained strong hurricane vortices as evident from the amplitude of max (V_t) at the starting time. The results for Hurricanes Bill and Gustav and the last case for Hurricane Earl (cases 8–10 in Table 1) were similar to the results in Fig. 2 (not shown). The consistency of short-term forecast spindown tendency among different cases and for different initial conditions suggest that the primary circulation intensity decline was an inherent feature of the short-term forecast for the high-intensity initial condition, irrespective of the origin of initial analysis.

Unlike for the high-intensity cases, the evolution of the axisymmetric primary circulation for the weaker intensity cases of Hurricane Earl (cases 1–2 in Table 1) in Figs. 3a and 3b shows that the intensity was increasing at all cycles in the forecast throughout the assimilation. Moreover, there were several cycles in which the analysis update reduced the prior forecast value. On the other hand, the amplitude of max(v) in Figs. 3d and 3e decreased in the forecast after an increase in the analysis, but at a smaller rate. Such evolution in the cycling resulted in a net gain of max(v) in the final analysis for these cases. Not surprisingly, the result suggests that the net gain in the axisymmetric primary circulation was required for the maximum absolute intensity to increase in the assimilation.

The primary circulation for the case of Hurricane Earl when it was a minimal category 3 storm (case 3 in Table 1) exhibited an evolution in the assimilation (Figs. 3c,f) that was a mix of weak and strong case behavior. For example, there was no net gain, relative to the first initial condition from the interpolated global analysis in either max(v) or max(V_t) within the lowest 2 km until the very last analysis update. The improvement in intensity was obtained in the last analysis because of observations within that cycle. An examination of the deterministic short-term forecast after the assimilation showed, however, an immediate spindown (not shown). Similar results were obtained for the cases of Hurricanes Bill and Gustav.

The overall impact of the spindown of the primary circulation during the assimilation was evaluated using the joint distribution of the change in circulation over the 1-h forecast and the update in the preceding analysis for all cases in Table 1 and all analysis cycles for each case. The joint distributions for the change in max(V_t) and max(v) are displayed in Fig. 4. The correlations computed from these joint distributions were -0.86 for max(V_t) and -0.79 for max(v). The large negative correlation indicates that the loss of primary circulation intensity due to the background forecast spindown was large on average. The spindown was especially large for the large updates in the analysis. To identify possible causes of the spindown forecast bias the evolution of pressure, storm size, and secondary circulation of the mean state were analyzed.

2) MSLP AND RMW

The evolution of MSLP and rmw in the assimilation revealed that for most cycles the spindown of primary circulation in the forecast was associated with a decrease in central pressure and vortex size in the core region. Examination of radial structure of the pressure field (not shown) indicated that the rate of pressure decrease was slightly higher away from the center than at the center, which resulted in a reduction of the radial pressure gradient near the rmw. Such tendency in the pressure field is consistent with a decrease in the gradient wind above the PBL. The results did not provide evidence that the spindown during the short-term forecast was characterized by a systematic imbalance between the primary circulation and mass field.

3) SECONDARY CIRCULATION

Analysis of the radial flow during the cycling was focused on the evolution within the PBL where the magnitude is the greatest in the vortex core region. Similar to the primary circulation results for the high-intensity cases of Hurricane Earl, the analysis update and the

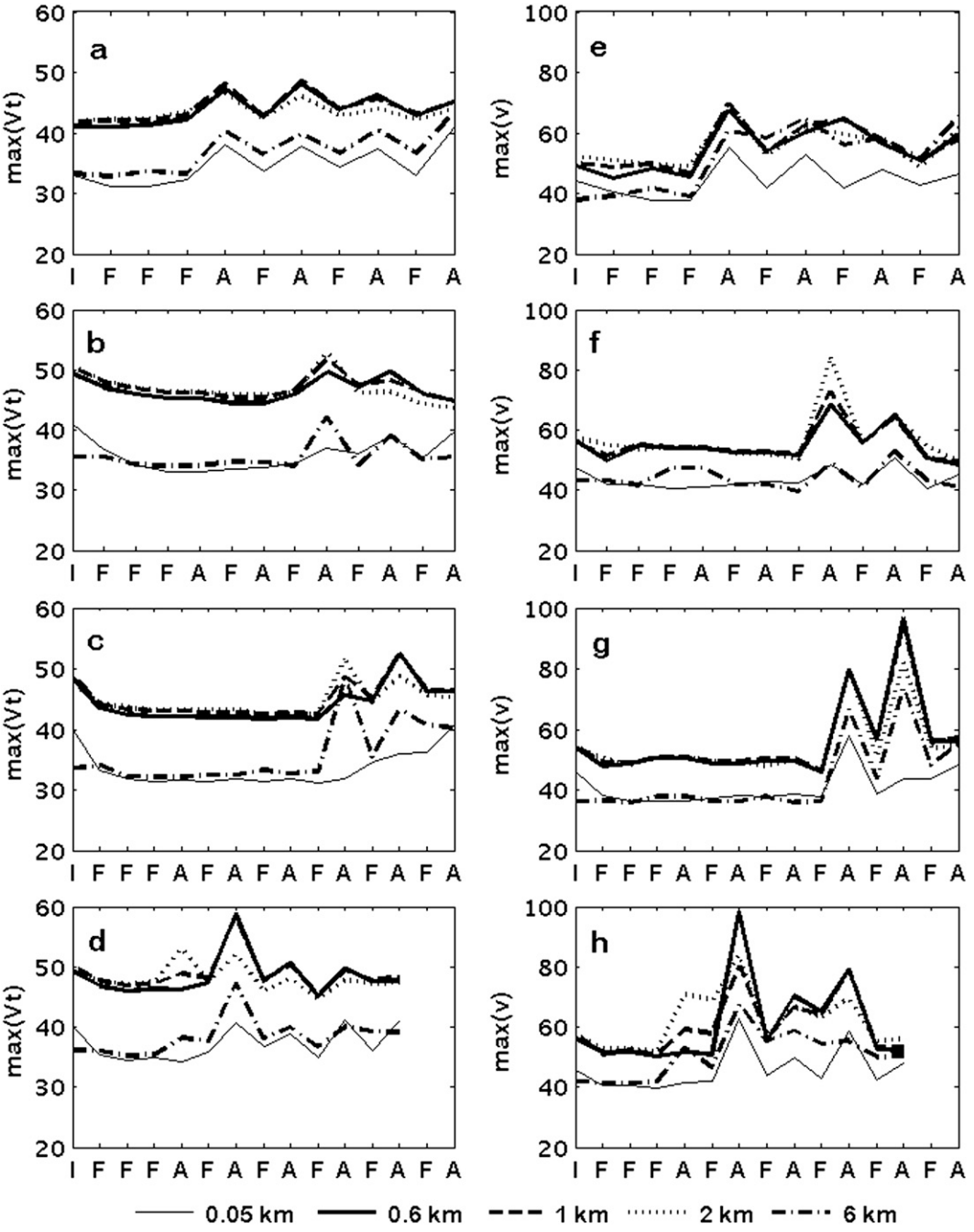

FIG. 2. (from top to bottom) Evolution of maximum (a)–(d) axisymmetric tangential velocity and (e)–(h) tangential velocity during cycling in HEDAS at the different vertical levels listed for high-intensity cases of Hurricane Earl. (a)–(d) Cases 4–7 and (e)–(h) the cases shown in Table 1. The units are m s^{-1}. On the horizontal axis, I is the starting time of the spinup period, F is the forecast, and A is the analysis instance at a frequency of 1 h.

change in subsequent forecast of the axisymmetric radial wind (V_{r^*}, defined in section 3) had the opposite tendency (Figs. 5a–d): the strength of the radial flow was decreased within PBL in the analysis updates and increased in the forecast. Moreover, the radial inflow at a height of 2 km was systematically changed toward positive values at the analysis update, indicating that the change from inflow to outflow at this height under the influence of observations. Unlike for the primary circulation, the weaker cases of Earl (Figs. 6a–c) in Table 1

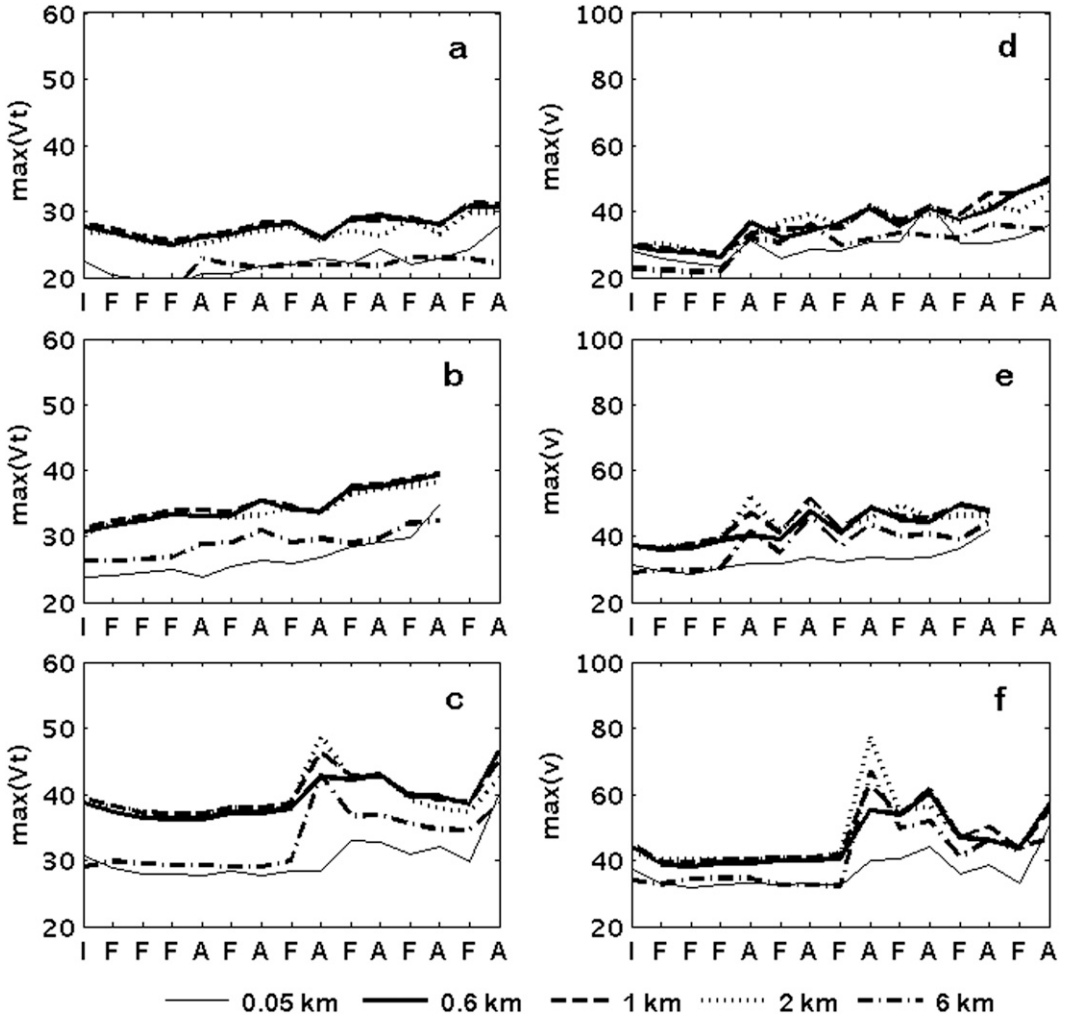

FIG. 3. As in Fig. 2, but for (a)–(c) weak-intensity cases of Hurricane Earl and (d)–(f) cases 1–3 in Table 1.

exhibited similar characteristics as the high-intensity cases (cf. Figs. 6a–c and 5a–d). The consistency of evolution of the radial flow during cycling among all cases suggests that the vertical structure of the secondary circulation within the PBL in the forecast was different from the observed structure, irrespective of the intensity and other properties for the different cases. Aksoy et al. (2013) show that maximum amplitude of inflow was underestimated with respect to the Doppler-based analysis for all cases. An examination of the inflow layer height (the diagnostic h_{PBL}, described in section 3) revealed that the PBL in the forecast was significantly deeper than in the analysis update. The frequency diagram of h_{PBL} for the prior forecast and posterior analysis for all cycles of the Earl experiments is displayed in Fig. 7. It is evident that the dominant inflow depth in the forecast was around 3 km, with a skewed distribution toward even higher values, whereas the distribution of h_{PBL} for the posterior analysis was more symmetrical and centered at about 2 km. The bias in inflow layer depth explains the persistent vacillations of V_{r^*} at every cycle toward and away from positive values, because the reversal of the radial flow in the background forecast was systematically occurring at higher vertical levels than in the observations. The significant difference in inflow layer depth and strength of V_{r^*} between the prior and posterior indicates that the forecast had a strong tendency to recover to the erroneously deep PBL within just 1 h. The observation-based estimates in J. A. Zhang et al. (2011) show an inflow-layer depth of about 1.5 km for the hurricane-strength TCs. The high bias of the inflow layer depth in the experimental HWRF model used in the current study was also documented in Bao et al. (2012).

The properties of the mean state evolution during the cycling are further analyzed in terms of the vertical

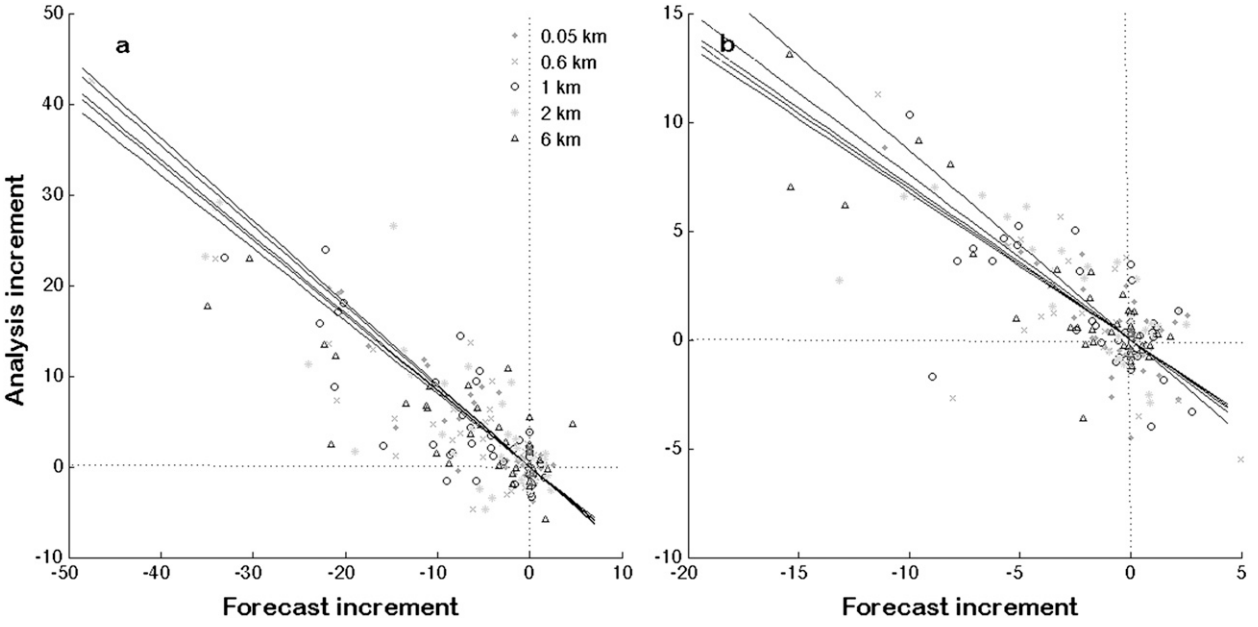

FIG. 4. Joint distribution between the change in amplitude of tangential velocity at the analysis update (vertical axis) and during subsequent 1-h forecast (horizontal axis) at the different vertical levels listed for all cycles of the cases in Table 1: maximum (a) tangential velocity and (b) axisymmetric tangential velocity. Units are $m\,s^{-1}$ for both axes.

component of the secondary circulation. The evolution of max(W) (defined in section 3) in the eyewall region is displayed in Figs. 5e–h for the high-intensity cases, corresponding to the radial flows diagnostic in Figs. 5a–d and the primary circulation in Fig. 2. The main property of max(W) in cycling was that the values increased in the forecast from exactly zero amplitude at initial times, including the beginning of the spinup period and all analysis updates. The zero value of vertical velocity at the analysis update is a direct consequence of the HWRF model formulation (Janjic 2003; Janjic et al. 2010). For this nonhydrostatic model the vertical velocity is formulated as a diagnostic variable that is advanced in the forecast based on prognostic hydrostatic and nonhydrostatic mass and horizontal wind variables. Such formulation implies that an appropriate nonhydrostatic vertical motion would result from the other initial state and forcing, such as convection, during a short-term forecast period.

The small amplitudes of max(W) in the forecast during the data assimilation in Figs. 5e–h indicate that neither the 1-h cycling period nor the 3-h forecast period prior to the assimilation were sufficient to evolve strong vertical motion that would be consistent with a mature hurricane ($W \approx 1$–$2\,m\,s^{-1}$; Rogers et al. 2012). Unlike during the initial period when the forecast evolved from the hydrostatic large-scale analysis, the short-term forecasts during the cycling with observations were initialized with nonhydrostatic horizontal wind, temperature, and mass analysis. The analysis included the nonhydrostatic state as was represented by the available observations, the forecast background and background error covariance. Clearly, such nonhydrostatic, mesoscale state was not sufficient to support immediate development of the strong vertical motion and convection in the eyewall for the hurricane cases. In contrast to the strong hurricane cases, the weaker intensity cases (the cases 1–2 in Table 1) exhibited a strong buildup of vertical velocity in the eyewall during cycling with the observations as shown in Figs. 6d and 6e. The amplitudes of max(W) at the end of the 1-h forecast were about 2 times higher than for the strong hurricane cases (Figs. 5e–h), and reached values close to $1\,m\,s^{-1}$ in some cycles. This result suggests that the rate of buildup of the secondary circulation and convection in the forecast during the assimilation was inversely proportional to the intensity. We hypothesize that such a relationship may arise from an inconsistency of the secondary circulation in the analysis updates with axisymmetric balance theory above the PBL (Shapiro and Willoughby 1982).

In a recent examination of tropical cyclone intensification, Bui et al. (2009) demonstrated that a general form of the Sawyer–Eliassen equation captures the majority of the axisymmetric component of the secondary circulation in a three-dimensional model with diabatic heating and frictional stress. In the PBL, where the balance assumption breaks down and an inward agradient force exists, the greatest departure from the balanced calculations is found. In the data assimilation

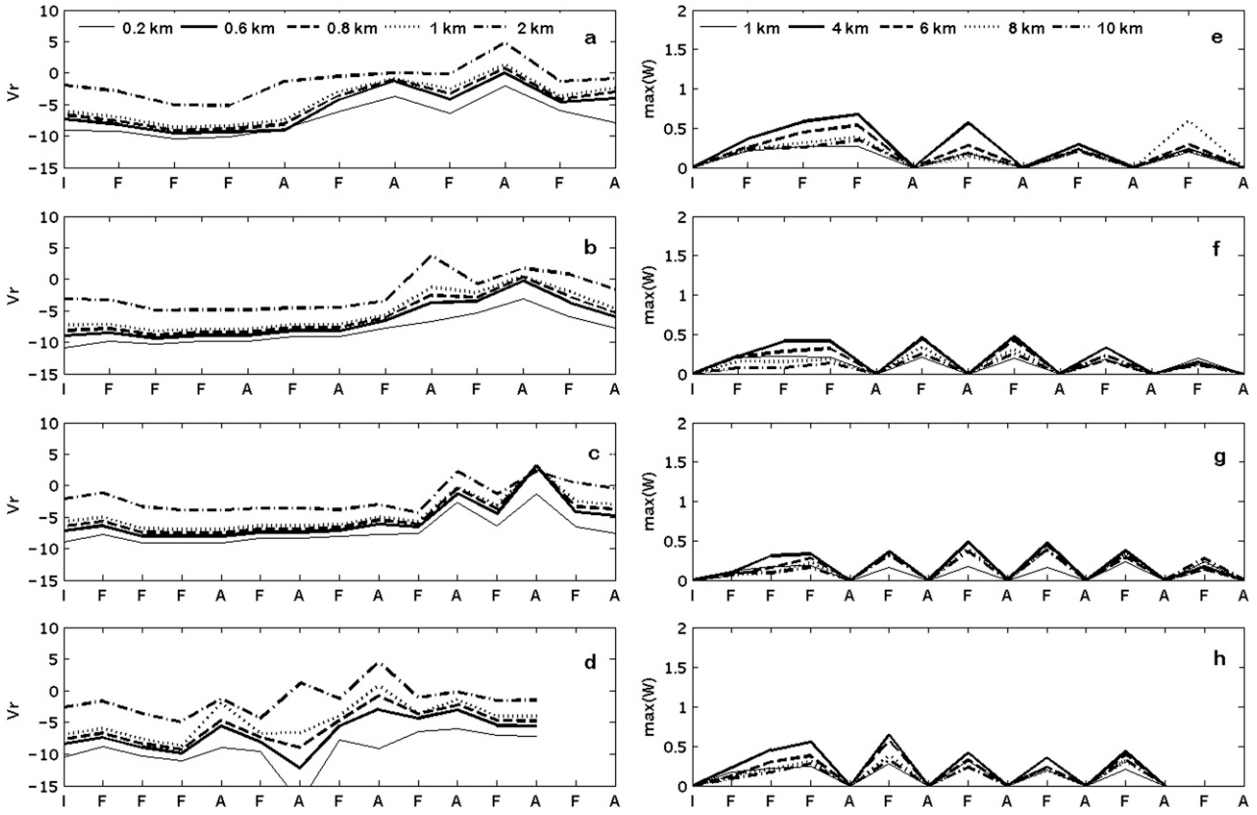

FIG. 5. As in Fig. 2, but for (a)–(d) axisymmetric radial velocity V_{r*} and (e)–(h) vertical velocity max(W).

experiments in this study the early transverse circulation in cases 1–2 could have been a close approximation to the balanced solution (above the PBL) consistent with the weaker primary circulation and early frictional stress and diabatic heating. Starting near such a balanced state might promote the early positive feedback between the intensification of convection and the primary circulation against the negative momentum flux. In contrast, for the

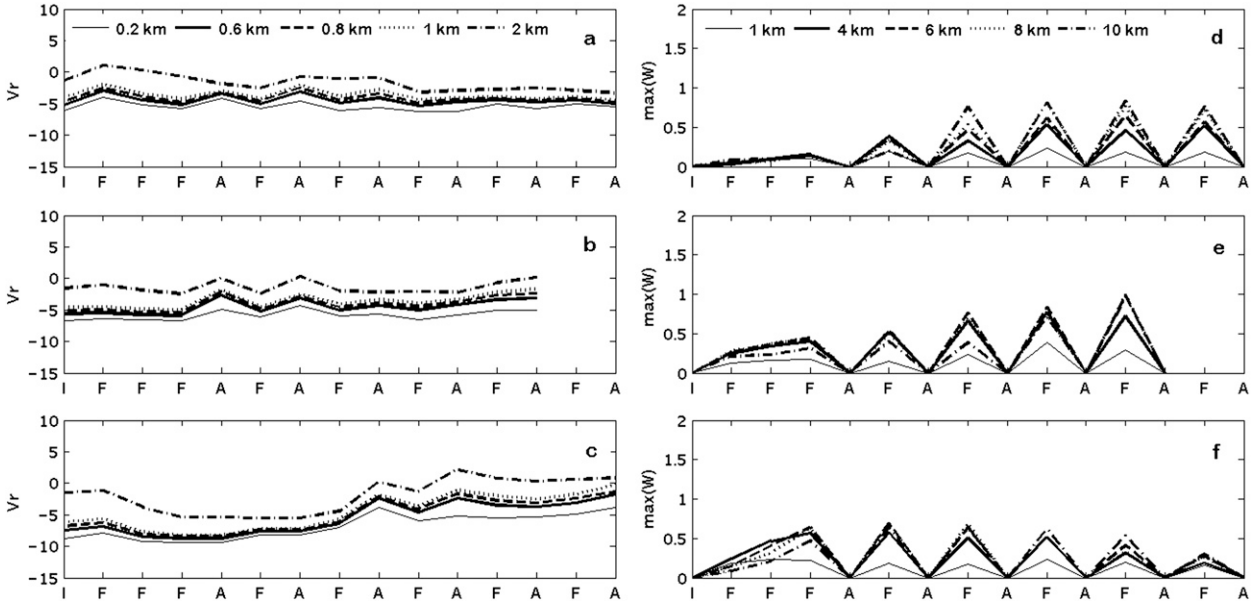

FIG. 6. As in Fig. 5, but (a)–(c) for weak-intensity cases of Hurricane Earl and (d)–(f) cases 1–3 in Table 1.

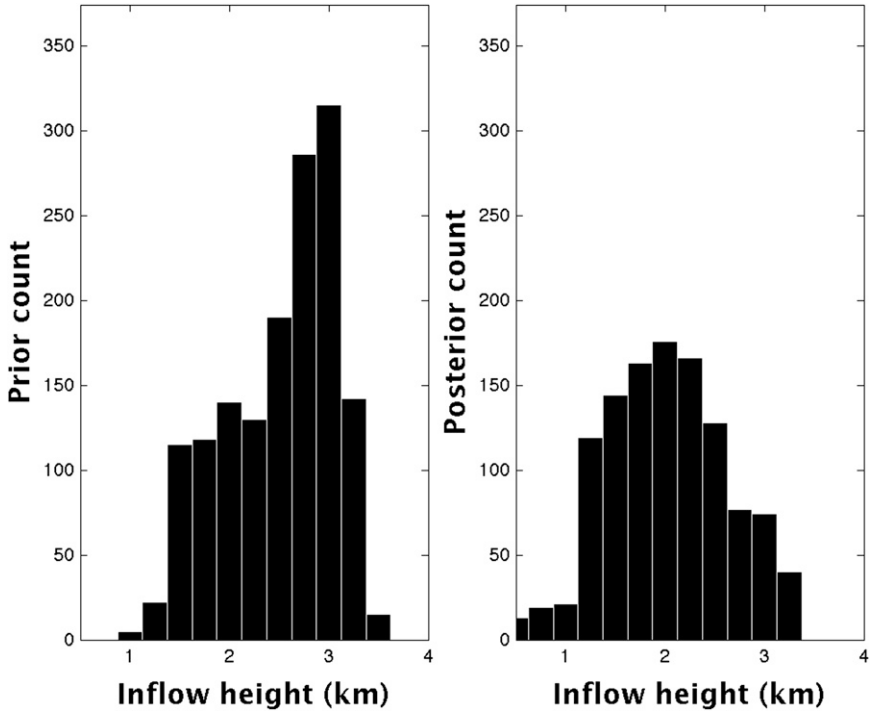

FIG. 7. Frequency distribution of inflow layer depth in the (left) prior forecast and (right) posterior analysis during cycling in HEDAS for the cases of Hurricane Earl (cases 1–7 in Table 1). The depth of the inflow layer is defined in section 3.

cases with high initial intensity, from the perspective of the balanced dynamics, a disconnect likely exists between the radial flow structure that is analyzed using observations and the weak vertical motion and diabatic heating that just start developing during the short-term forecast. The short-term forecast then evolves toward a state that is consistent with a mostly frictionally driven secondary circulation. Consequently, the primary circulation spins down through the impact of this negative momentum flux in the PBL and outflow above it. In this regime, the positive feedback between the primary circulation and convection could also apply but in the opposite sense of the weaker intensity cases: the weakening of the primary circulation was associated with suppressed convection, which in turn led to less forcing from the diabatic heating over the short forecast period of 1 h.

It is beyond the scope of this study to investigate the balanced solution and its use as a diagnostic tool in the examination of the mean circulation in the data assimilation cycling. This will be explored in future studies. The results in this study strongly suggest, however, that the spinup of vertical motion in the short-term forecast during cycling was not adequate for the high-intensity cases. This condition could be improved in the ensemble data assimilation by including new variables in the control state that would more directly affect the evolution of vertical motion during the cycling. A change of control variables in HEDAS will be addressed in future studies. To better understand the relationship between the updates in the primary circulation, which was well represented through the observations in the assimilation, and the vertical velocity, together with other variables that impact its evolution, in this study we examined the ensemble-based correlations using the axisymmetric representation of the state variables in the next section.

b. Analysis of background error correlations

A large majority of observations that were used in HEDAS consisted of horizontal wind information, including the flight-level and dropsonde horizontal wind vectors, SFMR-based near-surface wind speed, and a large volume of the Doppler radar radial velocities. Such observations naturally had the largest direct impact on updating the horizontal wind components above the PBL during the cycling, whereas the other variables were updated primarily by means of error covariance. As shown in the previous section, the vertical velocities were not updated in the analysis because of the model formulation. In the vortex-relative coordinate system, the observations projected mostly onto the primary circulation because the significant transverse circulation in the PBL was not well represented by the airborne

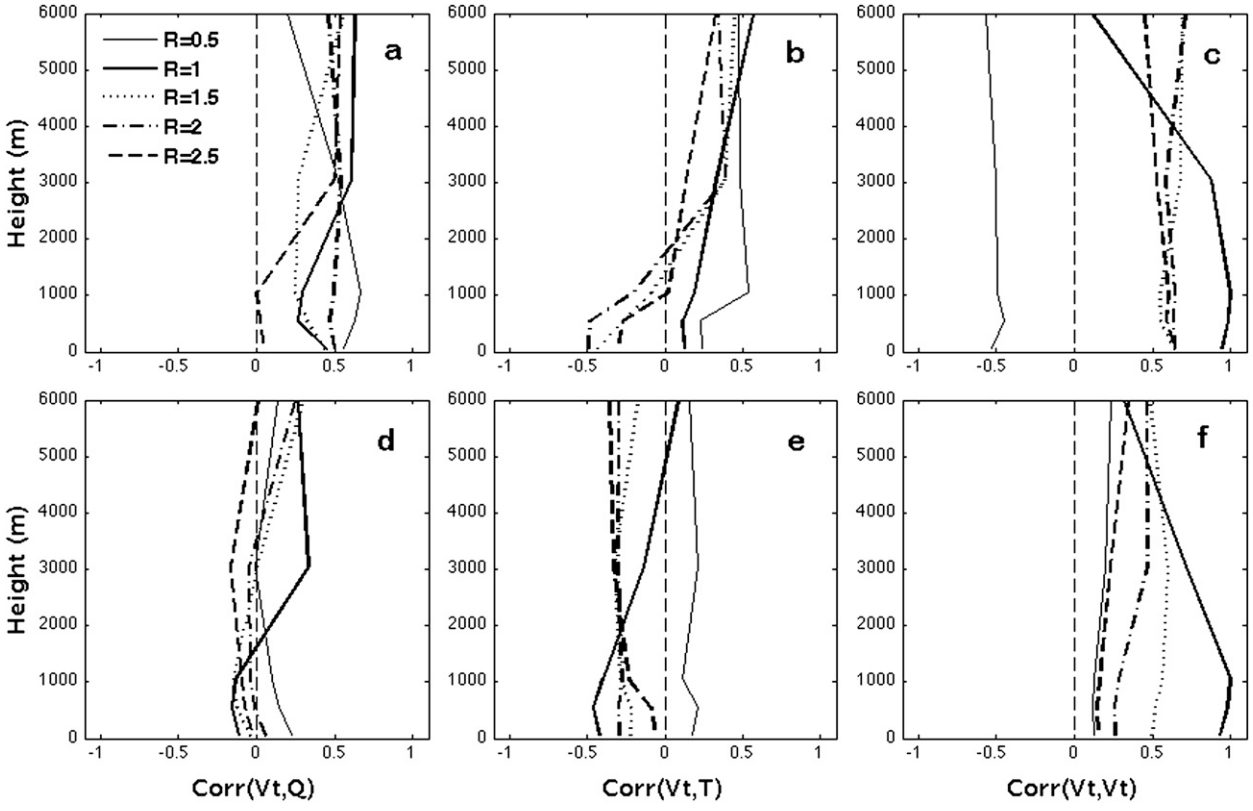

FIG. 8. Forecast-error correlations between axisymmetric tangential velocity V_t at the fixed location (r = rmw, h = 1 km) and (a),(d) axisymmetric humidity, (b),(e) axisymmetric temperature, and (c),(f) tangential velocity at different heights (vertical axis) and radii listed in the legend, for (top) weak and (bottom) strong intensity cases of Hurricane Earl. The diagnostic quantities used for computation of correlations are described in section 3.

observations. Only about 10% of observations were available above a height of 7 km and less than that below 1 km (Aksoy et al. 2013). Consequently, the error covariance of the primary circulation with other variables was considered the most significant to the update of unobserved vortex-relative state variables in the assimilation. In addition, because the ensemble covariance by definition represents a statistical estimate of the linearized relationship between the variations of variables that results from dynamical evolution over the short-term forecast period, examination of the properties of the covariance between the primary circulation and the other variables would aid in the interpretation of the dynamical relationship between them with respect to the dominant forecast tendency bias such as the spindown. In the following analysis, the correlations between the axisymmetric primary circulation V_t at a fixed location (r = rmw, h = 1 km) with axisymmetric temperature, humidity, and secondary circulation at several different (r, h) locations are presented.

For the weaker-intensity cases, which were characterized by an increase of the primary circulation in the forecast (Figs. 3a,b), the correlations with humidity were significant and positive in most regions and at all heights, especially within the eyewall region (Fig. 8a, for $0.5 \leq r \leq 2$). Such a distribution of correlations is consistent with the expected dynamical coupling for an intensifying vortex, where an increase in the primary circulation would be associated with an increase of humidity in the eyewall region. The background error correlations between V_t and temperature (Fig. 8b) were also consistent with the expected dynamical coupling for the intensifying vortex. Higher (lower) temperature in the eye was coupled with larger (smaller) V_t. This coupling between the variations of temperature and the primary circulation was especially strong above the PBL at heights above 2 km. In addition, the correlations with temperature outside the eyewall ($r > 1$) were positive above 1 km and negative below. This result implies that the increase in the primary circulation for the intensifying regime in the short-term forecast was associated with increasing temperatures above 1 km and decreasing temperatures below in the areas outside of the eyewall, which may have been

related to vertical mixing in the presence of convection in these regions.

The error correlation between the primary circulation and temperature and humidity for the high-intensity cases was smaller and of the opposite sign relative to the weaker cases in most regions (Figs. 8d,e). The reversal of the sign of correlations implies that the analysis update of the same sign in the primary circulation was associated with an update of temperature and humidity that was of the opposite sign between the strong and weak cases. It follows that an increase in primary circulation intensity by the impact of observations at the analysis update was associated with cooling and drying for the high-intensity cases and warming and moistening for the low-intensity cases.

Because the primary circulation was systematically weakened during the short-term forecast for the high-intensity cases (Fig. 2), the anticorrelated coupling between the variations of this circulation and temperature and humidity indicates that the erroneous forecast tendency (the tendency bias) caused positive feedback of errors in the cycling, which could not have been corrected by the wind observations alone. This hypothesis is consistent with the weak negative temperature bias in the final HEDAS analysis for the major hurricane cases (shown in Fig. 16c in Aksoy et al. 2013). Similarly, the higher positive error correlations in Figs. 8a and 8b for the weaker hurricane cases, are consistent with the strong warm bias in the final analysis for these cases (shown in Figs. 16a,b in Aksoy et al. 2013).

Regarding the dynamical mechanism of the spindown, the sign of the error correlations with temperature together with the condition that the spindown of the primary circulation was occurring in all ensemble members for the high-intensity cases, suggests that a decrease of temperature outside the eye region may have caused reduction of vertical momentum flux. The profiles of correlation between $V_t(r = \text{rmw}, z = 1\,\text{km})$ and $V_t(r, z)$ within the vortex core indicate weaker vertical and radial coupling of momentum for the strong cases (Fig. 8c) relative to the weak cases (Fig. 8d).

Examination of error correlations of the primary circulation with the vertical velocity for the high-intensity cases (not shown) suggested overall weak coupling between these fields during the spindown. The weak error correlations, less than 0.1 at heights above the PBL indicated that the vertical motion that was associated with delayed developing of convection did not have much influence on the primary circulation. In summary, the examination of background error correlations between the axisymmetric primary circulation and temperature, humidity, and vertical velocity in the vortex-relative framework indicated a dependence of these on the background forecast tendency bias. The results suggest that the spindown tendency error was reinforced during the cycling for the strong hurricane cases likely due to inconsistency of the secondary circulation in the analysis updates with the imposed strong primary circulation, coupled with the thermal and moisture biases that were not favorable to enhancing the evolution of secondary circulation during the short-term forecast.

5. Summary and conclusions

The encouraging results of prior studies on the impact of tropical cyclone (TC) vortex-scale assimilation of Doppler radar observations using the ensemble Kalman filter (EnKF) technique on intensity forecast skill suggested that improving the initial conditions at these scales with advanced data assimilation technology and high-resolution observations holds significant potential for making progress on the TC intensity forecast problem. To expand on that potential it is desirable to better understand the properties and sources of the uncertainty in the EnKF data assimilation at TC vortex scales with the high-resolution models.

In this study, we focused on the properties and origin of the systematic error component of the uncertainty with a special emphasis on the impact of background forecast bias during the assimilation. The Hurricane Weather Research and Forecasting (HWRF) Ensemble Data Assimilation System (HEDAS; Aksoy et al. 2013) was used. Unlike in the prior studies, this system was applied to all airborne observations from research and operational aircraft that were transmitted in real time, including the airborne Doppler radial wind speed, as in the prior studies, but also stepped-frequency microwave radiometer surface wind speed, and flight-level and dropwindsonde temperature, humidity, and wind measurements. Evaluation of the performance of HEDAS for 83 cases from 2008–11 using these observations is presented in detail in Aksoy et al. (2013). It was shown that overall HEDAS produced realistic analysis of TC states at vortex scales. HEDAS analyses were significantly better than the prior state without data assimilation. However, some systematic errors were identified in the analyses with respect to independent observation-based estimates. Most notably, relative to the independent Doppler-based wind analysis, the axisymmetric primary circulation intensity was underestimated for hurricane intensity cases and the secondary circulation was systematically weaker for all cases. Systematic errors were also noted for the estimates of temperature and humidity relative to the flight-level observations.

The analysis in this study of the evolution of the vortex state during the assimilation through cycling with the

observations shows that the low-intensity bias in the primary circulation for the hurricane cases was caused by the spindown of the entire vortex core circulation in the short-term forecast in each cycle. The spindown tendency was highly correlated with the intensity increase in the analysis updates with the observations, implying that the stronger intensity cases were associated with the largest loss of intensity in the short term forecast. The reoccurrence of spindown in the background forecast consequently resulted in virtually no net gain of the primary circulation intensity during the assimilation for the major hurricane cases. The spindown was also present in the ensemble forecasts prior to the beginning of assimilation, whenever the downscaled initial state from the global analysis already had a high-intensity vortex.

The spindown dynamical bias was associated with inadequate secondary circulation in the short-term forecast. Both the radial and vertical components of the secondary circulation were significantly weaker in these forecasts than expected for the strong primary circulation with observed organized convection. Consequently, the primary circulation could not be sustained. The diagnostic analysis indicates that the weak secondary circulation was the consequence of a combination of factors. First, the observations in the assimilation had limited information about the secondary circulation. Second, the forecast model exhibited a tendency to quickly recover to an erroneously deep PBL, implying a negative impact of too much vertical mixing on the structure of the radial circulation. Third, the short-range forecasts were initialized with zero vertical velocity in the assimilation cycling because of the standard formulation of the HWRF nonhydrostatic governing equations. The short forecast length during the assimilation did not allow enough time for the convection and the associated vertical circulation to develop completely. The development of vertical velocities was especially suppressed during the assimilation for the major hurricane cases. The influences of these factors were likely dependent on each other, implying that the systematic errors of in the forecast tendency were in a positive feedback with the systematic errors in the state.

The analyses of background error correlations of the axisymmetric primary circulation with the temperature and humidity revealed that the sign of correlations was dependent on the dynamical regime in the background forecast. The correlations were negative when the primary circulation was spun down and positive in the opposite regime. This result implies that in the analysis updates the increase in the primary circulation tended to cool and dry the vortex state for the high-intensity cases and warm and moisten the weak-intensity cases. These results are consistent with the temperature and humidity biases in the final analysis. The dependence of correlations on the forecast tendency indicates that the systematic errors of poorly observed quantities were strongly linked to the forecast tendency bias. The quantities that were poorly observed were temperature, humidity, and secondary circulation especially in the PBL.

Considering that currently available observations are limited regarding the state of the secondary circulation within the TC vortex, the results recommend including the additional constraints in the vortex-scale data assimilation, such as the Sawyer–Eliassen equation above the PBL, to improve the representation of the secondary circulation and the associated initial forecast tendency. In addition, more observations of temperature and humidity are desirable in order to reduce the background state biases, including the impact of those on the background error correlations. Improvements to the model used in the data assimilation are expected to also have positive impact on the analysis, together with advances in data assimilation aspects. These could include adjustment of spatial localization scales to reflect properties of multiscale vortex structure, and use of additional control variables that would directly influence the secondary circulation. Future studies with HEDAS would include testing the impact of these factors.

Regarding the impact of vortex-scale data assimilation on the prediction of TC intensity using high-resolution models with EnKF or similar techniques, the findings in this study indicate that the systematic errors in the analysis that are linked to the forecast tendency bias would lead to the short-term forecast bias after the assimilation for the same reasons. The findings of weak or no improvement of short-term forecast skill in prior studies could be explained in terms of such bias.

Acknowledgments. The authors thank the HRD modeling group, especially Drs. Xuejin Zhang and Thiago Quirino, for invaluable support for the experimental HWRF. Thanks to Dr. Michael Montgomery for many insightful discussions that helped guide the diagnostic analyses. The authors would also like to thank Drs. Robert Rogers and Sundararaman Gopalacrishnan for their constructive comments on earlier versions of the manuscript. This study was partially supported through funding from the NOAA Hurricane Forecast Improvement Project (HFIP) and the HFIP computing resources.

REFERENCES

Aberson, S. D., 2010: 10 years of hurricane synoptic surveillance (1997–2006). *Mon. Wea. Rev.,* **138,** 1536–1549.

——, M. L. Black, R. A. Black, R. W. Burpee, J. J. Cione, C. W. Landsea, and F. D. Marks Jr., 2006: Thirty years of tropical cyclone research with the NOAA P-3 aircraft. *Bull. Amer. Meteor. Soc.,* **87,** 1039–1055.

Aksoy, A., S. Lorsolo, T. Vukicevic, K. J. Sellwood, S. D. Aberson, and F. Zhang, 2012: The HWRF Hurricane Ensemble Data Assimilation System (HEDAS) for high-resolution data: The impact of airborne Doppler radar observations in an OSSE. *Mon. Wea. Rev.,* **140,** 1843–1862.

——, S. D. Aberson, T. Vukicevic, K. J. Sellwood, S. Lorsolo, and X. Zhang, 2013: Assimilation of high-resolution tropical cyclone observations with an ensemble Kalman filter using NOAA/AOML/HRD's HEDAS: Evaluation of the 2008–11 vortex-scale analyses. *Mon. Wea. Rev.,* **141,** 1842–1865.

Bao, J.-W., S. G. Gopalakrishnan, S. A. Michelson, F. D. Marks, and M. T. Montgomery, 2012: Impact of physics representations in the HWRFX on simulated hurricane structure and pressure–wind relationships. *Mon. Wea. Rev.,* **140,** 3278–3299.

Berg, R. J., and L. A. Avila, 2011: Atlantic hurricane season of 2009. *Mon. Wea. Rev.,* **139,** 1049–1069.

Bui, H. H., K. R. Smith, M. T. Montgomery, and J. Peng, 2009: Balanced and unbalanced aspects of tropical-cyclone intensification. *Quart. J. Roy. Meteor. Soc.,* **135,** 1715–1731.

Davis, C., and Coauthors, 2008: Prediction of landfalling hurricanes with the Advanced Hurricane WRF Model. *Mon. Wea. Rev.,* **136,** 1990–2005.

Emanuel, K., 2005: *Divine Wind: The History and Science of Hurricanes.* Oxford University Press, 296 pp.

Gall, R., J. Franklin, F. Marks, E. N. Rappaport, and F. Toepfer, 2013: The Hurricane Forecast Improvement Project. *Bull. Amer. Meteor. Soc.,* **94,** 329–343.

Gamache, J. F., 1997: Evaluation of a fully three-dimensional variational Doppler analysis technique. Preprints, *28th Conf. on Radar Meteorology,* Austin, TX, Amer. Meteor. Soc., 422–442.

Gaspari, G., and S. E. Cohn, 1999: Construction of correlation functions in two and three dimensions. *Quart. J. Roy. Meteor. Soc.,* **125,** 723–757.

Gopalakrishnan, S. G., and Coauthors, 2002: An operational multiscale hurricane forecasting system. *Mon. Wea. Rev.,* **130,** 1830–1847.

——, N. Surgi, R. Tuleya, and Z. Janjic, 2006: NCEP's two-way-interactive-moving-nest NMM-WRF modeling system for hurricane forecasting. Preprints, *27th Conf. on Hurricanes and Tropical Meteorology,* Monterey, CA, Amer. Meteor. Soc., 7A.3. [Available online at https://ams.confex.com/ams/27Hurricanes/techprogram/paper_107899.htm.]

——, F. Marks Jr., X. Zhang, J.-W. Bao, K.-S. Yeh, and R. Atlas, 2011: The experimental HWRF system: A study on the influence of horizontal resolution on the structure and intensity changes in tropical cyclones using an idealized framework. *Mon. Wea. Rev.,* **139,** 1762–1784.

Hamill, T. M., J. S. Whitaker, M. Fiorino, and S. J. Benjamin, 2011a: Predictions of 2010's tropical cyclones using the GFS and ensemble-based data assimilation methods. *Mon. Wea. Rev.,* **139,** 3243–3247.

——, ——, D. T. Kleist, M. Fiorino, and S. J. Benjamin, 2011b: Global ensemble predictions of 2009's tropical cyclones initialized with an ensemble Kalman filter. *Mon. Wea. Rev.,* **139,** 668–688.

Janjic, Z. I., 2003: A nonhydrostatic model based on a new approach. *Meteor. Atmos. Phys.,* **82,** 271–285.

——, R. Gall, and M. E. Pyle, 2010: Scientific documentation of the NMM solver. NCAR Tech. Note NCAR/TN-477+STR, 210 pp. [Available from the National Center for Atmospheric Research, P.O. Box 3000, Boulder, CO 80307-3000.]

Lorenz, E., 1969: The predictability of a flow which possesses many scales of motion. *Tellus,* **21,** 289–307.

Montgomery, M., and S. K. Smith, 2011: Paradigms for tropical-cyclone intensification. *Quart. J. Roy. Meteor. Soc.,* **137,** 1–31.

Poterjoy, J., and F. Zhang, 2011: Dynamics and structure of forecast error covariance in the core of a developing hurricane. *J. Atmos. Sci.,* **68,** 1586–1606.

Rappaport, E. N., 2009: Advances and challenges at the National Hurricane Center. *Wea. Forecasting,* **24,** 395–419.

Reasor, P. D., M. D. Eastin, and J. F. Gamache, 2009: Rapidly intensifying Hurricane Guillermo (1997). Part I: Low-wavenumber structure and evolution. *Mon. Wea. Rev.,* **137,** 603–631.

Rogers, R., S. Lorsolo, P. Reasor, J. Gamache, and F. Marks, 2012: Multiscale analysis of tropical cyclone kinematic structure from airborne Doppler radar composites. *Mon. Wea. Rev.,* **140,** 77–99.

Rotunno, R., and C. Snyder, 2008: A generalization of Lorenz's model for the predictability of flows with many scales of motion. *J. Atmos. Sci.,* **65,** 1063–1076.

Shapiro, L. J., and H. E. Willoughby, 1982: The response of balanced hurricanes to local sources of heat and momentum. *J. Atmos. Sci.,* **39,** 378–394.

Snyder, C., and F. Zhang, 2003: Assimilation of simulated Doppler radar observations with an ensemble Kalman filter. *Mon. Wea. Rev.,* **131,** 1663–1677.

Weng, Y., and F. Zhang, 2012: Assimilating airborne Doppler radar observations with an ensemble Kalman filter for convection-permitting hurricane initialization and prediction: Katrina (2005). *Mon. Wea. Rev.,* **140,** 841–859.

Whitaker, J. S., and T. M. Hamill, 2002: Ensemble data assimilation without perturbed observations. *Mon. Wea. Rev.,* **130,** 1913–1924.

Xiao, Q., Z. Zhang, C. Davis, J. Tuttle, G. Holland, and P. J. Fitzpatrick, 2009: Experiments of hurricane initialization with airborne Doppler radar data for the Advanced Research Hurricane WRF (AHW) model. *Mon. Wea. Rev.,* **137,** 2758–2777.

Zhang, F., Y. Weng, J. F. Gamache, and F. D. Marks, 2011: Performance of convection-permitting hurricane initialization and prediction during 2008-2010 with ensemble data assimilation of inner-core airborne Doppler radar observations. *Geophys. Res. Lett.,* **38,** L15810, doi:10.1029/2011GL048469.

Zhang, J. A., R. F. Rogers, D. S. Nolan, and F. D. Marks, 2011: On the characteristic height scales of the hurricane boundary layer. *Mon. Wea. Rev.,* **139,** 2523–2535.

Zhang, X., T. Quirino, K.-S. Yeh, S. Gopalakrishnan, F. Marks, S. Goldenberg, and S. Aberson, 2011: HWRFx: Improving hurricane forecasts with high-resolution modeling. *Comput. Sci. Eng.,* **13,** 13–21, doi:10.1109/MCSE.2010.121.